J Mater Sci (2008) 43:350–356
DOI 10.1007/s10853-006-1237-7

Changes in microfibril angle in cyclically deformed dry coir fibers studied by in-situ synchrotron X-ray diffraction

Klaus J. Martinschitz · Peter Boesecke · Christopher J. Garvey · Wolfgang Gindl · Jozef Keckes

Received: 7 September 2005 / Accepted: 31 January 2006 / Published online: 2 December 2006

Abstract Dry coir fibers are characterized by wide-angle X-ray scattering coupled with tensile tests. The fibers exhibit elastic and plastic behavior with the yield point at a strain of about 2%. In-situ experiments document that the cyclic loading and unloading beyond the yield point does not reduce the stiffness of the fibres, since they recover their initial stiffness by every increase of the strain. The diffraction data show that the microfibril angle (MFA) of cellulose fibrils in the coir fibre cells is inversely proportional to the magnitude of the applied strain. In average, the relatively high MFA of about 45° in the unstrained state decreases linearly upon straining until the fibers break at about 35% strain. When the strain is released during the tensile experiment the MFA tends to recover its original magnitude. No significant differences in the dependence of MFA on strain are detected in elastic and plastic regions, respectively. The results demonstrate that the tissue with helical architecture does not have to be saturated with water in order to exhibit the effect of the recovery of the mechanical function when cyclically loaded. This indicates differences in the architecture of the coir cell wall in comparison with that of compression wood with high MFA whereby similar phenomena were observed in the wet state.

K. J. Martinschitz · J. Keckes (✉)
Erich Schmid Institute of Materials Science, Austrian Academy of Sciences and Institute of Material Physics, University of Leoben, Jahnstrasse 12, 8700 Leoben, Austria
e-mail: keckes@unileoben.ac.at

P. Boesecke
European Synchrotron Radiation Facility, Grenoble, France

C. J. Garvey
Australian Nuclear Science and Technology Organisation, Menai, Australia

W. Gindl
Department of Materials Science and Process Engineering, University of Natural Resources and Applied Life Sciences, Vienna, Austria

J. Keckes
Materials Center Leoben Forschung GmbH, Leoben, Austria

Introduction

Coir is a lignocellulosic fruit fiber obtained from the fibrous mesocarp of coconuts, the fruit of the coconut palm (*Cocos nucifera*). With a world production of about 250,000 tons, it is extensively cultivated in tropic countries like India and Sri Lanka.

Coir is a multicellular fiber bundle, which consists of 30–300 cells in its cross-section. Cells are composed of about 32–43% partly crystalline and helically arranged cellulose, and a non-crystalline matrix consisting of 40–45% lignin, and pectin [1]. Coir fibers exhibit valuable physical properties like high fracture strain and toughness [2], which make the coir fiber interesting for various domestic and commercial applications [3–6].

Up to now, most of the structural studies of coir were performed using X-ray scattering in static conditions or at distinct elongations. Small-angle X-ray scattering (SAXS) on coir fibers indicated a decrease of the microfibril angle (MFA) from 45 to 25° when the fiber was stretched from 0 to 115% in an alkali solution [7]. The influence of various thermal and mercerization

treatments on the changes in the chemical and structural properties of the coir fibers was reported [8].

It was demonstrated that the elastic modulus of coir fibers depends on the fiber diameter and on MFA [2]. Similarly as other lignocellulosics, also in the case of coir the helical angle of the cellulose fibrils in the cell wall, the cellulose texture, predefines the stress–strain behavior. Since coir fibers exhibit relatively high MFA, a high fracture strain of up to 30% was reported [2]. These parameters resemble the behavior of compression wood from spruce branches, whereby the high MFA in the S_2 layer results in a high extensibility of the tissue along the direction of the cell axis [9, 10]. In the case of wood, MFA magnitude is a consequence of structure optimization and tissues from different trees exhibit very comparable mechanical properties provided the MFAs are comparable [11, 12].

Recently, significant effort has been dedicated to study the properties of cellulosics and lignocellulosics using time-resolved synchrotron scattering coupled with mechanical tests [12–16]. It has been demonstrated that the orientation distribution function of cellulose fibrils in wet composites produced by the bacterium *Acetobacter xylinu*s is a function of the external strain regardless of the presence or absence of xyloglucan or pectin applied as a matrix [13]. Similarly, experiments on wet samples of compression wood have documented that the MFA magnitude decreases linearly with the strain increase while this effect is pronounced especially beyond the yield point [12, 16]. The behavior was exclusively observed in the case of wet wood samples while dry samples of compression wood showed relatively small decrease of the MFA and small fracture strain. The data from wet wood tissues have additionally indicated that the slopes of unload and loading curves as well as the slope of the stress–strain curve observed shortly after the experiment was interrupted and subsequently continued coincide approximately with the slope of stress–strain dependence in the elastic region [12, 16]. This was related to the molecular mechanistic effects acting on the molecular and submolecular levels and originating in the interfacial interaction of the polymers. It was supposed that these Velcro-like phenomena originate in the interaction between the crystalline cellulose fibrils and the amorphous matrix of lignin and hemicellulose [12].

As documented above, predominantly wet conditions and relatively simple mechanical tests have been applied to analyze the properties of the cellulosics. For the understanding of structure–property relationship in these complex hierarchical tissues, however, the phenomena occurring during cyclic testing are of significant importance. The main aim of the present work is to study the properties of *dry coir fibers* applying *cyclic tensile loading and unloading* in order (1) to analyze the effect of the water presence on the mechanical and structural response of the helical tissue and (2) to evaluate the influence of cyclic loading beyond the yield point on the MFA magnitude. Since coir is usually used in dry conditions, the study should provide also useful information for the practical application of the tissue. One of the goals is to compare the behavior of coir and wood, since coir cells have an architecture comparable to compression wood tracheids.

Experiment

Coir fibers of *C. nucirefa* with a length of about 60 mm and a homogeneous diameter in the range 0.08–0.5 mm were selected. The fiber diameters were determined in an optical microscope analyzing the cross-sectional area at both ends using ImageJ image analysis software [17]. The typical diameter of the fibers was about 200 μm. The fibers were glued between two flexible wood plates at both ends and then mounted between aluminum grips of a self-made computer-controlled tensile stage mechanically identical with that used in Ref. [12]. The fixing of the fibers using wood plates was important to avoid the slipping and damage of the fibers in and by the metal grips, respectively. The software controlling the stage enabled to perform complex strain-controlled experiments like cyclic loading, straining with different speeds, quick increase or decrease of the straining etc. The actual strain of the fibers was determined by means of a video extensometry using a digital camera and microscope.

The force on the fiber was monitored by a load sensor the signal of which was collected by an analog-digital card integrated into the computer. The fibers were tested at ambient conditions whereby the moisture content determined by oven-drying was approximately 12–15%. Tests were made also with the fibers inserted before the experiment for 1 h into water of 25 °C though no new features in the behavior of these fibers were observed in comparison with the behavior of those tested under ambient conditions. Further on, only the data from the fibers tested under ambient conditions—dry coir fibers are presented.

The structural changes in the fibers during the tensile experiments were characterized by in-situ wide-angle X-ray scattering (WAXS). The experiments were performed at ID01 beamline of European synchrotron radiation facility (ESRF) in Grenoble, France. For the

experiment, the radiation with the wavelength of 0.082 nm and a two dimensional (2D) detector with 1,024 × 1,024 pixels were used. To collect one 2D detector image, the time of about 5.5 s was needed. The beam size on the sample was approximately 0.5×1 mm^2. The sample-detector distance was set to 96 mm. The detector was mounted asymmetrically in order to observe a significant part of the cellulose 004 Debye-Scherer ring besides that of cellulose 200. The structural data were used to evaluate the magnitude of MFA (with the precision of ±1°) from the azimuthal positions of cellulose 200 reflections using the procedure described elsewhere [18]. The fibers were strained with the speed of 0.01 mm/s corresponding to the step of about 1.4×10^{-4}s^{-1}of the strain. This was a compromise allowing to collect a relevant number of WAXS images during one mechanical test. Tests were made also with the speeds of 0.001 and 0.1 mm/s, though no additional rate effects were observed. The force direction was always parallel to the fiber axis.

About 20 fibers of different diameter were tested in a tensile stage while collecting WAXS patterns using 2D detector. The experiments were technically very complicated since the synchronization of various tasks and computers was necessary. One of the most serious practical problems appeared to be a movement of the fiber out from the beam what caused the loss of the structural information. For the mechanical testing three different straining procedures were used, namely (1) the samples were strained by a continuous increase of the strain until the fracture occurred, (2) the straining was interrupted few times and then continued and (3) the loading direction was few times reversed until zero stress was detected and then the straining continued.

Results and discussions

Morphology of coir fibers was characterized using scanning electron microscopy (SEM). In Fig. 1, a representative SEM micrograph of a coir fracture surface is presented. It is possible to recognize tubular cells oriented parallel with the bundle axes. Moreover, one can notice that the fracture of individual helical cells results in the formation of curled triangular features indicating a specific fracture mechanism.

Practically all fibers investigated exhibited very comparable MFAs in the unstrained state of approximately 45°. Due to straining, the MFA decreased in all fibers. In Fig. 2a, b an example of WAXS patterns collected at the beginning and at the end (before fracture) of a representative in-situ experiment are presented. The results in Fig. 2 clearly document a

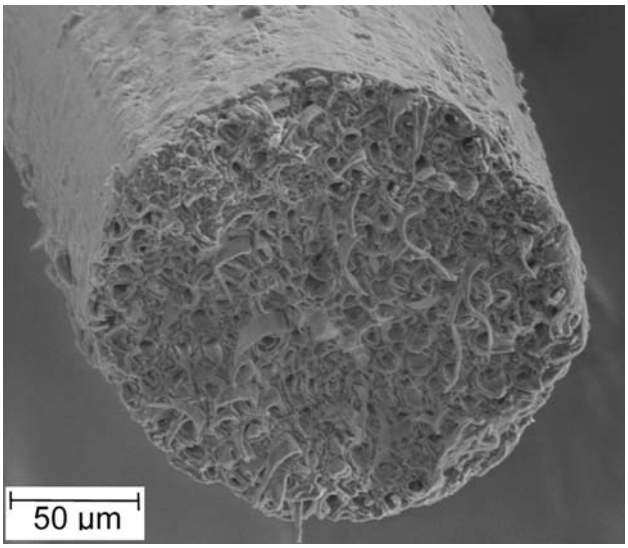

Fig. 1 Representative scanning electron micrograph of a coir fracture surface (magnification ×500). One can recognize individual cells in the bundle as well as curled triangular rests of cell walls indicating a specific fracture mechanism of the helical tissue

significant change in the texture of the cellulose fibrils due to straining. In Fig. 3a and b, the integrated data obtained from Figs. 2a and 1b, respectively, are presented. The curves (Fig. 2) represent an azimuthal distribution of intensity along Debye-Scherer rings of cellulose 200 reflections (Fig. 2) and document a decrease of MFA from 43 to 27°.

In Fig. 4, mechanical and structural data, namely the stress–strain curve (a) and the dependence of MFA on the applied strain (b), collected during a representative tensile experiment on a dry coir fiber, are presented. In the stress–strain dependence, one can identify an elastic behavior up to the strain of about 2%. Around this value plastic deformation sets in. By contrast to tensile experiments with compression wood, whereby an increase of the slope of the stress–strain curve towards the end of the experiment was reported, the slope remained constant until fracture in the coir fiber. The results indicate that the magnitude of MFA is a linear function of the strain applied with approximately $MFA(\varepsilon) = 43 - 45*\varepsilon$. This is in agreement with data collected from compression wood [12] where a similar relationship was observed. However, one cannot observe different slopes in the MFA dependence on strain in the elastic and plastic regions respectively, as it was reported for *Cryptomeria japonica* [16]. A theoretical dependence $MFA(\varepsilon) = MFA(0) - \cot(MFA[0])*\varepsilon$ derived for the behavior of idealized helical structure is also included in Fig. 4b [12]. In contrast with the data in Fig. 4b, the dependence

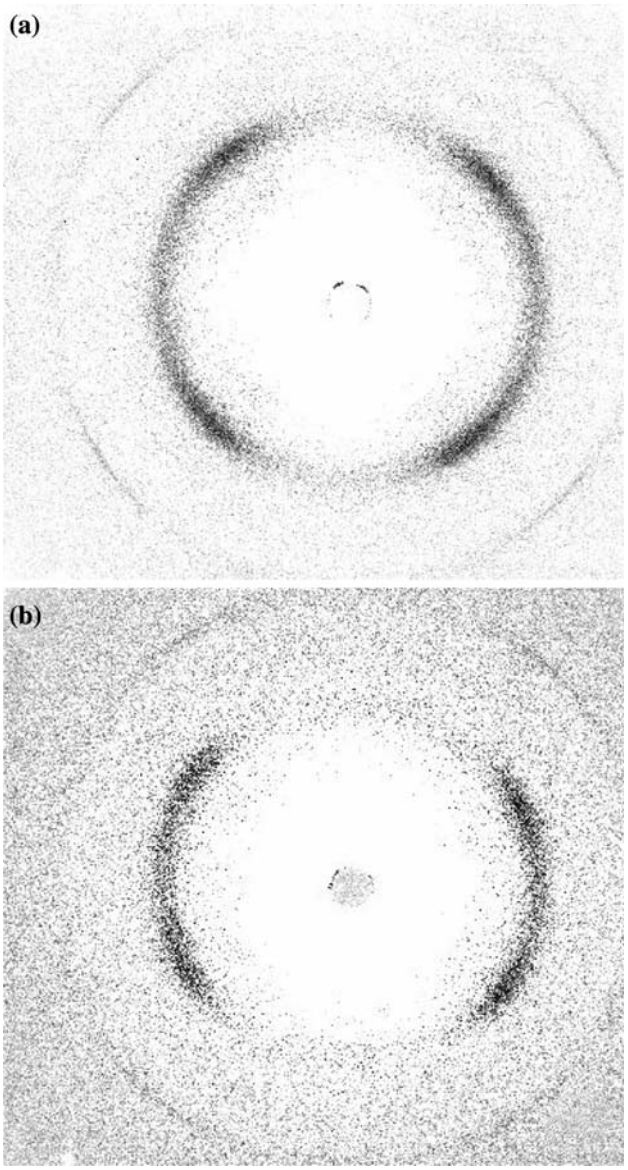

Fig. 2 Results from WAXS on a coir fiber. The patterns(**a**) and (**b**) collected at the beginning and at the end of the in-situ experiment, respectively, demonstrate a decrease of MFA in the fibre from 46 to 31°

predicts more pronounced decrease of MFA with the strain increase what documents that not all structural changes accompanying the deformation of the coir fiber are accommodated by the reversible decrease of MFA.

In Fig. 5, results from a tensile experiment whereby the straining was five times interrupted for 1 min are presented. By the continuation of the straining after a holding period of 1 min, approximately the same initial elastic modulus is observed for all straining steps (Fig. 5a). At the end of the experiment, an increase of the slope can be recognized which can be interpreted as the alignment of the cellulose fibrils in the force

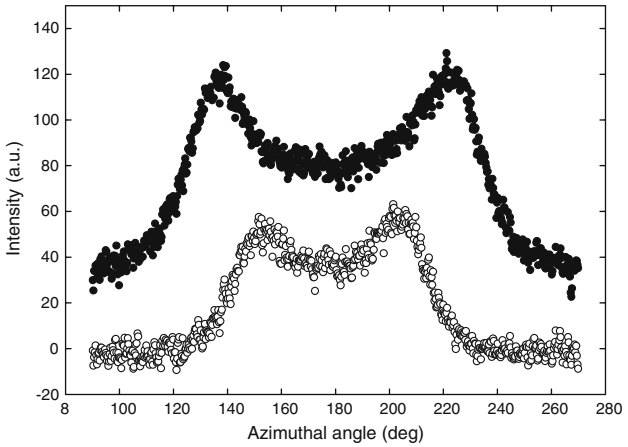

Fig. 3 Results from WAXS on a coir fibre. *Filled* and *empty symbols* represent integrated data from Fig. 1a and b, respectively. The data demonstrate a decrease of MFA due to straining

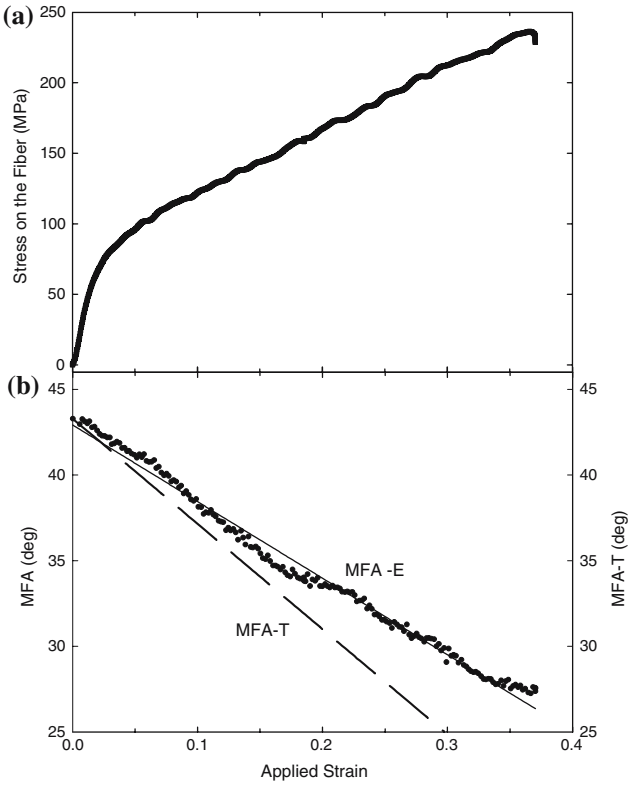

Fig. 4 Mechanical (**a**) and structural data (**b**) from in-situ WAXS experiments on a coir fibre. The stress–strain curve shows a biphasic behaviour with elastic and plastic region. In (**b**) the corresponding experimental dependence (MFA-E) of the MFA as a function the strain is depicted by points. The *solid line* in (**b**) represents a the linear fit of the data yielding MFA(ε) = 43 – 45*ε. The *dashed line* (MFA-T) corresponds to an idealized theoretical dependence of MFA on strain, namely MFA(ε) = MFA(0) – cot(MFA[0])*ε, derived for the behavior of idealized helical structure [12]

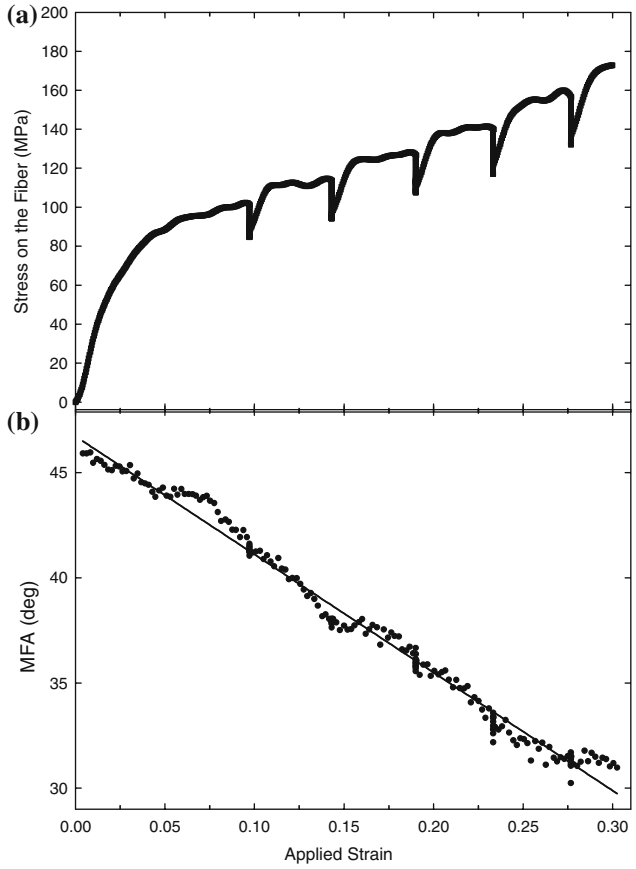

Fig. 5 Mechanical and structural data from in-situ WAXS experiments on a coir fibre. The stress–strain curve in (**a**) documents that the straining of the fiber was five times interrupted. In (**b**) the corresponding dependence of the MFA as a function the strain is depicted by points. The *solid line* in (**b**) represents the linear fit of the data yielding MFA(ε) = 48 – 56*ε

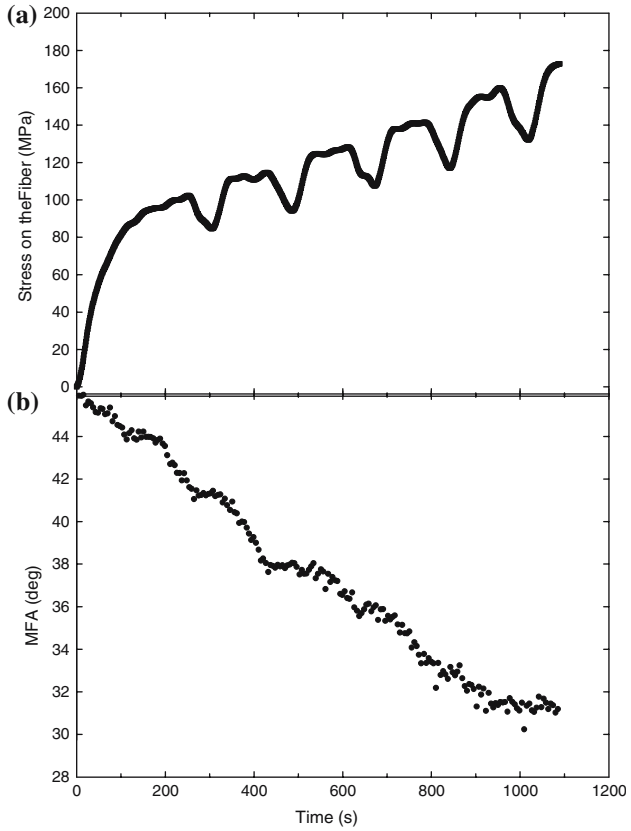

Fig. 6 Stress (**a**) and MFA (**b**) data from Fig. 5 plotted as a function of time. The data indicate an exponential relaxation of the stress (**a**) and a slight increase of MFA (**b**) when the straining was interrupted

direction. In Fig. 5b, the approximately linear dependence of MFA on the strain can be recognized with MFA(ε) = 48 – 56*ε. Again there is no difference in the MFA(ε) slope in the elastic and plastic region. The data in Fig. 5 are practically identical with those obtained from compression wood of *Picea abies* [L.] Karst. Also the idealized theoretical dependence MFA(ε) = MFA(0) – cot(MFA[0])*ε [12] derived for the behavior of the compression wood fits excellent in this case. What is however interesting is the fact that the tissue was tested at ambient conditions in dry state compared to the experiments with compression wood [12, 16], which were always performed with water saturated tissues. In spite of this, the effect of the stiffness recovery observed in wet compression wood occurs also in dry coir fiber and indicates thus that the tissue can adapt the strain and recover its mechanical function after plastic deformation. In Fig. 6, the data from Fig. 5 are presented against time in order to obtain more insight into time-dependent effects. In the case of stress, one can identify a relaxation when the straining was interrupted especially for the first, third and fifth straining step. The dependence of MFA on time (Fig. 6b) documents that the MFA is constant or even slightly increases when the straining is interrupted, what is a new observation which was not reported in the case of compression wood.

In Fig. 7, the results of a new type of experiment whereby a dry coir fiber was repeatedly loaded and unloaded are presented. Similar to the behavior of metals, the decrease of the strain in the plastic region induces a decrease of the stress. Upon loading, as the strain is put back, the fiber shows a modulus which is comparable with that observed in the elastic region when the experiment started. When the stress magnitude approaches the point where the strain was released, however, again the plastic deformation occurs. The envelope of the stress–strain curve observed in Figs. 3and 4 is also in this case preserved and the slope in the plastic region is not influenced by the cycling procedure. The dependence of MFA on

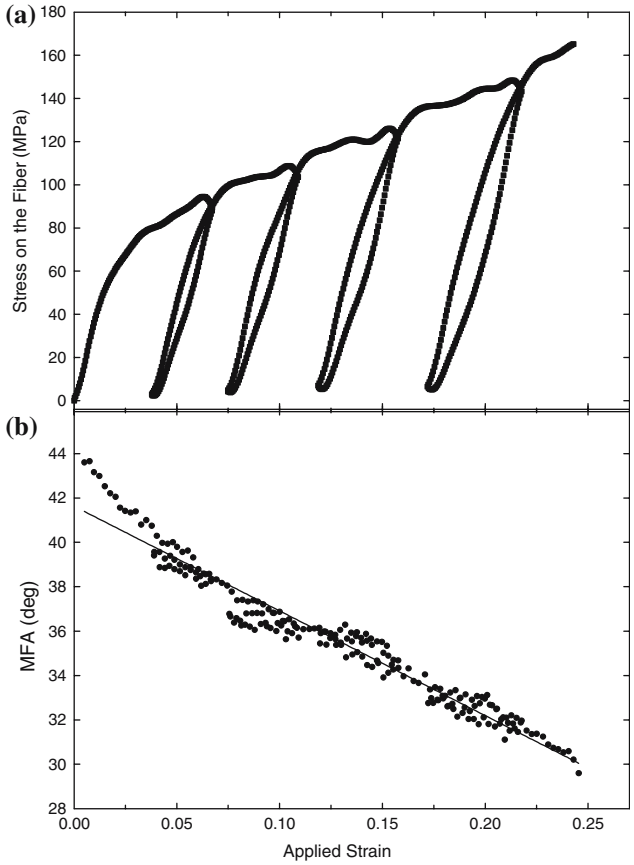

Fig. 7 Mechanical and structural data from in-situ WAXS experiments on a coir fibre. The stress–strain curve in (**a**) documents that, in the plastic region, the strain was four time reduced and subsequently increased. In (**b**) the corresponding dependence of the MFA as a function the strain documents that, when strain is released, the MFA tends to recovery the original value. The *solid line* in (**b**) represents the linear fit of the data yielding MFA(ε) = 42 – 47*ε

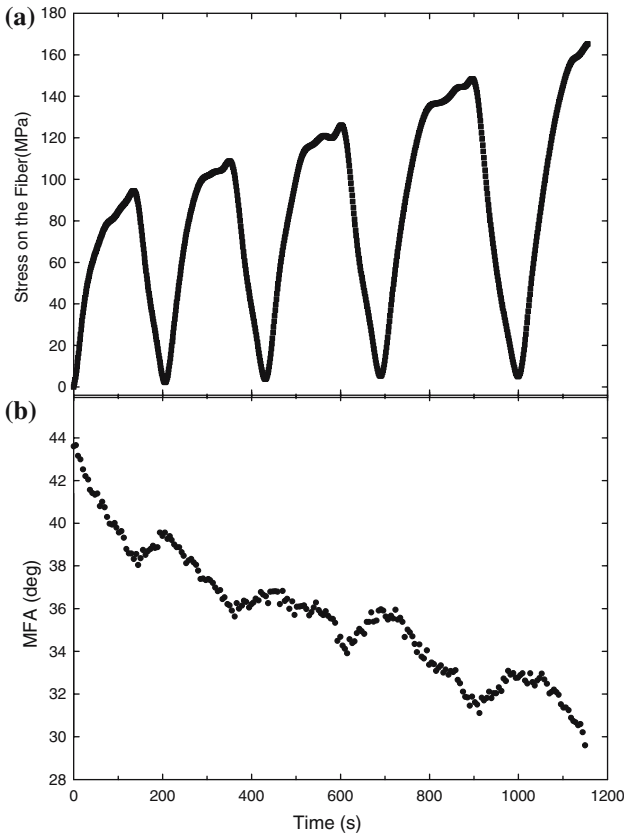

Fig. 8 Stress (**a**) and MFA (**b**) data from Fig. 7 plotted as a function of time. The data indicate that, when the fiber was unloaded, the MFA increased

strain (with MFA(ε) = 42 – 47*ε) this specific experiment (Fig. 7a) indicates at first a relatively steep decrease of the MFA up to the point when the stress is first time released. From that point, MFA(ε) slope is not so pronounced. When unloading and loading back, MFA increases and decreases, respectively, but the absolute magnitude is not fully recovered. In other words, when the strain is decreased the MFA does not reproduce exactly its original magnitude. The increase of the MFA magnitude by sample unloading is more obvious from Fig. 8 whereby Fig. 8a shows the stress on the fiber as a function of time and Fig. 8b documents the MFA behavior. Another obvious information in Fig. 8 resides in the fact that the MFA magnitude is not correlated with the stress values but only with the actual strain imposed on the sample.

The MFA dependence on strain observed in the coir fibers is comparable with the behavior cells of compression wood [12]. The helical angle is inversely proportional to the tissue extension and the tissues behave like a spring. The release of the strain causes, in approximation, the recovery of MFA. Interestingly, the mechanical response of the tissue depends on the specific stage of the tensile experiment. When the straining is interrupted or the strain is released, the tissue exhibits a recovery of the mechanical function. Up to now, however, such behavior was reported only for various compression wood types namely, *Ginkgo biloba* L., *Juniperus virginiana* L., *P. abies* [L.] Karts and *C. japonica* [12, 16], which were saturated by water. Here, it is shown for the first time that also coir fibers characterized at ambient conditions with the moisture in the range 12–15% can exhibit stiffness recovery behavior. The present results thus relativise the importance of the tissue saturation by water in the mechanical performance of tissues with helical architecture. Even relatively dry coir fibers exhibit high fracture strain, stiffness recovery effects and decrease of MFA upon stretching. This clearly indicates that the mechanics of the lignocellulosic helical tissues is predetermined by the unique architecture of the cell

wall whereby the nature of the mechanistic interaction of crystalline and amorphous constituents is of outmost importance. The presence of lignin, hemicellulose and pectin in the non-cellulosic cell wall matrix and, above all, the presence of adsorbed water can contribute to those effects. The key to understand the role of the water in the helical tissue resides in the understanding of the difference in the nanostructural properties between the cells of coir and compression wood. Then the exact function, the nature and the position of the cross links in the helical cell wall can be identified.

Conclusions

The novelty of this work can be summarized as follows:

1. Dry coir fibers were tested by in-situ synchrotron X-ray scattering coupled with tensile testing. The helical tissues were cyclically loaded in the tensile stage and the structural data were characterized using WAXS. The fibers exhibit the recovery of the mechanical function during unloading and loading experiments.
2. The magnitude of MFA in the fibers is approximately inversely proportional to the strain applied with approximately $MFA(\varepsilon) = MFA(0) - \cot(MFA[0])*\varepsilon$. When the strain on the fiber is released, MFA tends to recover its original value.
3. The results document the helical tissue does not have to be saturated by the water in order to exhibit the effect of the recovery of the mechanical function when cyclically loaded. This indicates significant differences in the architecture of the cell wall of coir and compression wood.

References

1. Bismarck A, Mishra S, Lampke T (2005) In: Mohanty AK, Misra M, Drzal LT (eds) Natural fibers, biopolymers, and biocomposites. Taylor and Francis, Boca Raton, pp 37
2. Kulkarni AG, Satyanarayana KG, Sukumaran K, Rohatgi PK (1981) J Mater Sci 16:905
3. Pavithran C, Gopakumar K, Prasad SV, Rohatgi PK (1981) J Mater Sci 16:1548
4. Roe PJ, Ansell MP (1985) J Mater Sci 20:4015
5. Bisanda ETN, Ansell MP (1992) J Mater Sci 27:1690
6. Geethamma VG, Reethamma J, Sabu T (1995) J Appl Pol Sci 55:583
7. Roy SC, Das S (1965) J Appl Pol Sci 9:3427
8. Mahato DN, Mathur BK, Bhattacherjee S (1993) J Mater Sci 28:2315
9. Meylan BA, Butterfield BG (1978) Wood Sci Technol 12:219
10. Navi P, Rastogi PK, Gresse V, Tolou A (1995) Wood Sci Technol 29:411
11. Reiterer A, Lichtenegger H, Tschegg S, Fratzl P (1999) Philos Mag A 79:2173
12. Keckes J, Burgert I, Frühmann K, Müller M, Kölln K, Hamilton M, Burghammer M, Roth SV, Stanzl-Tschegg S, Fratzl P (2003) Nat Mater 2:810
13. Astley OM, Donald AM (2001) Biomacromol 2:672
14. Astley OM, Chanliaud E, Donald AM, Gidley MJ (2003) Int J Biol Macromol 1636:1
15. Crawshaw J, Bras W, Mant GR, Cameron RE (2002) J Appl Pol Sci 83:1209
16. Kamiyama T, Suzuki H, Sugiyama J (2005) J Struct Biol 151:1
17. http://www.rsb.info.nih.gov/ij/
18. Lichtenegger H, Reiterer A, Stanzl-Tschegg SE, Fratzl P (1998) In: Microfibril angle in wood, proceedings of the IAWA/IUFRO international workshop on the significance of microfibril angle to wood quality, Westport, New Zealand, p 140